Measurement of thermal properties of biological tissues and tissue-mimicking phantom with a dual-needle sensor

Leonardo Bianchi
Department of Mechanical Engineering, Politecnico di Milano
Milan, Italy
leonardo.bianchi@polimi.it

Somayeh Asadi
Department of Mechanical Engineering, Politecnico di Milano
Milan, Italy
somayeh.asadi@polimi.it

Martina De Landro
Department of Mechanical Engineering, Politecnico di Milano
Milan, Italy
martina.delandro@polimi.it

Sanzhar Korganbayev
Department of Mechanical Engineering, Politecnico di Milano
Milan, Italy
sanzhar.korganbayev@polimi.it

Paola Saccomandi
Department of Mechanical Engineering, Politecnico di Milano
Milan, Italy
paola.saccomandi@polimi.it

2022 IEEE International Symposium on Medical Measurements and Applications (MeMeA) | 978-1-6654-8299-8/22/$31.00 ©2022 IEEE | DOI: 10.1109/MEMEA54994.2022.9856408

***Abstract*—This work presents the measurement of the thermal properties of *ex vivo* biological tissues (i.e., porcine liver and kidney tissues) as a function of temperature, along with the thermal characterization of a tissue-mimicking agar-based phantom. The evaluation of the thermal properties was performed by the dual needle technique, adopting a sensor equipped with two needles, capable to deliver thermal energy to the biomaterial and monitor the related tissue thermal behavior. Measurements of thermal conductivity, thermal diffusivity, and volumetric heat capacity were conducted at room temperature and at temperatures relevant from a biological point of view, namely, body temperature and temperatures of ~60 °C- 65 °C, which are typically correlated to instantaneous thermal damage in tissue. Thermal properties of biological tissue remained rather constant at the investigated temperatures: average values of thermal conductivity ranged from 0.515 W/(m·K) to 0.575 W/(m·K), thermal diffusivity ranged from 0.144 mm²/s to 0.163 mm²/s, whilst the average volumetric heat capacity was from 3.48 MJ/(m³·K) to 3.72 MJ/(m³·K). Furthermore, the thermal properties of the realized agar phantom were comparable to the ones of biological tissues. The results of this study provide valuable information for the characterization of porcine liver and kidney tissues, in terms of their thermal properties, to be used in predictive mathematical models of thermal therapies and validate the usage of agar phantoms as tissue-mimicking materials.**

Keywords—thermal properties, biological tissue, tissue-mimicking phantom, liver, kidney, dual-needle technique

I. Introduction

The measurement of the physical properties of tissues of biological origin represents a crucial aspect for several areas of biomedical engineering [1]. These areas range from the research intended to realize tissue-mimicking phantoms, i.e., materials that mimic the characteristics of biological media and are worthwhile for the testing and improvement of medical systems [2]–[6], to the characterization of tissue properties aimed at optimizing diagnostic and therapeutic procedures [7], [8]. In this regard, the study of the thermal properties of biological tissues assumes a pivotal role as these properties regulate the way heat distributes within tissue, thus, they are involved in all therapies which entail a variation of the tissue temperature to treat a disease [8]. Thermal therapies, namely radiofrequency ablation [9], microwave ablation [10], laser ablation [11], [12], high focused ultrasound [13], and cryoablation [14], have been introduced as minimally invasive procedures exploiting a temperature increment or decrement (as in case of cryoablation) to induce the desired thermal damage in the unhealthy tissue area [15]. Promising results have been attained in terms of reduction of the operative trauma and hospitalization times compared to traditional surgical approaches. However, toward the further amelioration of thermal techniques, the prediction of the heat distribution and subsequent temperature variation in tissue is required to prevent excessive thermal damage to healthy tissue while assuring the complete eradication of the diseased tissue. Hence, to assess the thermal outcome at given procedural settings and precisely plan the thermal therapy, computational frameworks have been proposed as they can simulate the temperature distribution and related tissue injury [16]–[18], provided that accurate information of the tissue thermophysical properties is given. Thus, experimental investigations are needed to determine tissue thermal properties, such as thermal conductivity (k), tissue specific heat capacity (c), the volumetric heat capacity (c_v) and thermal diffusivity (D), to be included in the simulation tools [19], [20]. The k denotes the ability of tissues to conduct heat, the tissue c concerns the heat necessary to increment the temperature of tissue by 1 °C per mass unit, and it is related to c_v by means of the tissue density ρ (i.e., $c_v = \rho c$). Furthermore, the thermal diffusivity D describes the capability of tissue to conduct heat in relation to its heat storage characteristics since it is expressed as the ratio between k and c_v: $D = k/c_v$ [19], [21], [22].

Different techniques have been utilized to measure the tissue thermal properties and characterize the thermal behavior of biomaterials. The self-heated thermistor technique, which relies on the use of a single thermistor probe, has been employed to assess D and k of different biological

This project has received funding from the European Research Council (ERC) under the European Union's Horizon 2020 research and innovation programme (Grant agreement No. 759159). This work was also funded by Fondazione Cariplo (grant n° 2017-2075).

media [23], [24]. Moreover, analyses with differential scanning calorimetry have been performed to investigate the specific heat capacity of tissues as well as the transition temperatures of biological components [25], [26]. Lastly, the so-called dual-needle technique has been adopted for the measurement of k, D, and c_v by means of a dual-needle sensor located into tissue, allowing for both the heating of tissue and temperature monitoring [19], [20], [27]–[29]. Further evaluations are necessary to outline the thermal characteristic of tissues that are targets of thermal therapies. In this concern, this work presents the measurement of thermal properties of porcine liver and kidney tissues, as a function of different selected temperatures, based on the usage of a dual-needle sensor. Furthermore, the same measurement technique has been utilized to characterize the thermal properties of an agar-based phantom, in order to compare its thermal properties to the ones of biological tissues.

II. Materials and Methods

A. Experimental protocol

Porcine liver and kidney tissues, excised from healthy animals, were attained from a local butcher. Tissue samples were cut from the entire organs and accurately placed in a metallic container, then positioned in a water thermal bath (Fig. 1.A). The thermal bath (temperature range from 20 °C to 100 °C, temperature fluctuation: 0.5 °C, rated wattage of 200 W, capable of a fast ramp-up from 20 °C to 37 °C in 10 min) was used to increase and control the tissue temperature up to specific values. The galvanized container was employed to prevent the water-tissue direct interaction while allowing the necessary heat transfer from the water of the thermal bath to the tissue specimen. For each biological tissue type, thermal properties were estimated by the so-called dual-needle technique, adopting a dual-needle sensor and a thermal property analyzer (as described in the following section II.B), at different temperatures. The selected temperatures were: *i*) room temperature, *ii*) temperatures close to body temperature, and *iii*) ~60 °C - 65 °C (i.e., temperatures relevant in thermal therapies since tissue thermal damage is typically instantaneous at 60 °C and above it). Besides the dual-needle sensor, which allows for both temperature monitoring and estimation of thermal properties, two additional sensors were used to measure the tissue temperature. A k-type thermocouple (0.1 °C accuracy) was embedded in a first needle, whereas an array of 10 Fiber Bragg Grating (FBG) thermometers (FiSens GmbH, Braunschweig, Germany), inscribed in a single-mode polyimide-coated optical fiber (1550 nm wavelength operation range) was inserted in a second metallic 18 G needle (1.2 x 50 mm). The FBG sensors (1 mm edge-to-edge distance, 1 mm sensing length) were illuminated by an optical spectrum interrogator (Micron Optics si255, Atlanta, USA, 1 pm accuracy corresponding to 0.1 °C), and their optical response was analyzed to monitor the temperature [30], [31]. These two needles were placed in tissue approximately at the same radial distance from the center of the specimen at which the needles of the dual-needle sensor were located. This is useful to provide information on the spatial temperature distribution in the sample since the tissue surrounding the dual-needle sensor must reach the thermal equilibrium condition prior to proceeding with the measurement of thermal properties.

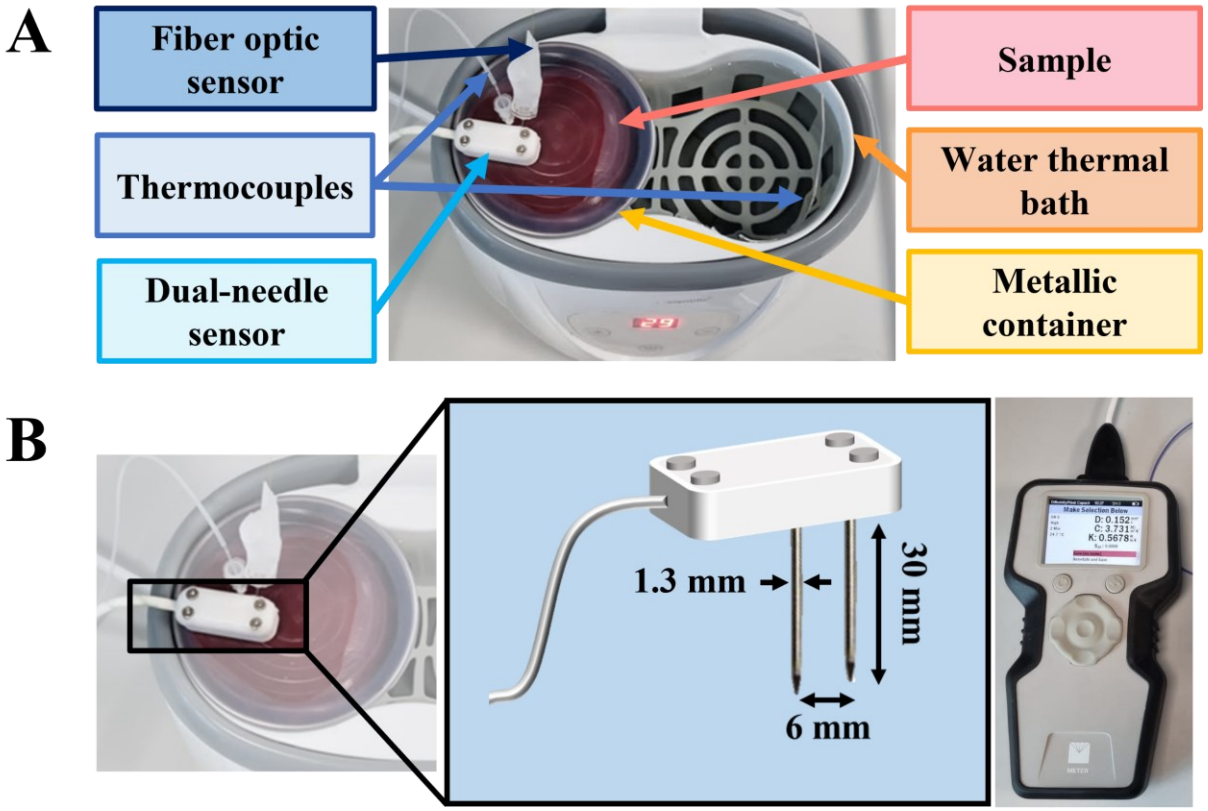

Fig. 1. (A) Experimental setup involving a water thermal bath to impose the selected temperature to the specimen, temperature sensors to monitor the temperature of the sample and water, a metallic container in which the sample is positioned, and the dual-needle sensor. (B) Dual-needle sensor (left) and thermal property analyzer (right) utilized for the measurement of thermal conductivity, thermal diffusivity, and volumetric heat capacity of the biological tissues and agar-based phantom.

An additional k-type thermocouple (0.1 °C accuracy) was used to monitor the water temperature. Overall, the experimental protocol consisted in: imposing the selected tissue temperature with the thermal bath; verifying that the water temperature matched the imposed one; assessing the effective tissue temperature, and proceeding with the measurement of the thermal properties at the selected temperature. The measurements were repeated 3 times for each tissue and for each temperature value.

Regarding the thermal characterization of the tissue-mimicking phantom, the thermal properties of an agar-based phantom were measured through the dual-needle technique. To synthesize the phantom, agar powder was dissolved in distilled water to attain a solution with a concentration of 2.5% [4]–[6]. A hotplate stirrer was used to mix the solution and increase its temperature. Particular attention was devoted to preventing evaporation while assuring that the powder was entirely dissolved. After removal from the hotplate, the sample was left at room temperature in order to solidify [4], [5]. The thermal properties of the realized phantom were assessed at the same temperatures chosen for the evaluation in *ex vivo* biological tissues. Also in this case, thermal property measurements at each temperature value were performed in triplicates.

B. Measurement of thermal properties with dual-needle technique

The measurement of the thermal properties (thermal conductivity, thermal diffusivity, and volumetric heat capacity) of *ex vivo* biological tissue and the agar-based phantom was performed by means of a dual-needle sensor (TEMPOS SH-3, range -50 °C – 150 °C), connected to a thermal property analyzer (TEMPOS, Meter Group, Inc., Pullman, WA, USA, 10% accuracy) by a flexible cable. The specifications of the dual needle sensor are the following: the two parallel metallic needles are 30 mm in length, with a diameter of 1.3 mm, and 6 mm distance between each other (Fig. 1.B). The dual-needle probe was accurately placed in the biological tissue or the phantom assuring that the two needles were directly in contact with material under study, prior to starting the experimental trial.

The mechanism at the basis of the dual needle technique consists in providing thermal energy to the biomaterial under examination by applying a certain current to one of the two needles of the sensor, which is called heating needle, for a time equal to 30 s (t_h). The second needle, called monitoring needle, allows the measurement of the temperature during the heating time and for the following 90 s. By subtracting the initial material temperature to the reached thermal value, the temperature rise ΔT can be calculated. The following equations are then employed by the thermal property analyzer to attain the values of thermal conductivity (k) and diffusivity (D) by means of the least-squares method [19], [20]:

$$\Delta T = \left[\frac{q}{4\pi k}\right] E_i\left[\frac{-r^2}{4Dt}\right] \qquad t \le t_h \tag{1}$$

$$\Delta T = \left[\frac{q}{\pi k}\right]\left\{E_i\left[\frac{-r^2}{4D(t-t_h)}\right] - E_i\left[\frac{-r^2}{4Dt}\right]\right\} \qquad t > t_h \tag{2}$$

being q the amount of heat provided by the heating needle, while E_i is the exponential integral [32], r is the distance between the two needles of the sensor, and t is the time. The volumetric heat capacity (c_v) is then obtained by the formula $c_v = k/D$ [19].

C. Measurement uncertainty

The measurement uncertainty was estimated in conformity with the guidelines of the "Guide to the expression of uncertainty in measurement" [33], to provide an indication of the quality of the attained experimental results. Therefore, in the following, when reporting the average values of the measured thermal properties (i.e., k, D, and c_v) for the *ex vivo* biological tissues and the tissue-mimicking phantom, also the measurement uncertainty will be specified, according to (3):

$$y_{T_{set}} = \overline{y_{T_{set}}} \pm U = \overline{y_{T_{set}}} \pm k_f \cdot s \tag{3}$$

being y_{Tset} the thermal property measured at the selected temperature T_{set}, $\overline{y_{T_{set}}}$ is the arithmetic mean of results of n measurements performed at the temperature T_{set}, U indicates the expanded measurement uncertainty, k_f is the coverage factor, and s refers to the standard uncertainty. U is attained by the product of k_f and s. The coverage factor k_f is calculated, considering a Student's t-distribution, with a 95% confidence level, for $n = 3$ (degrees of freedom equal to 2), therefore k_f is equal to 4.30. Moreover, s, which is related to measurement repeatability, is defined as the standard deviation of the mean, expressed as:

$$s = \sqrt{\frac{\sum_{i=1}^{n}\left(y_{T_{set,i}} - \overline{y_{T_{set}}}\right)^2}{n(n-1)}} \tag{4}$$

being $y_{Tset,i}$ the thermal property measured in the i-th measurement performed at the selected temperature $T_{set.}$

III. Results and Discussion

The results attained for each thermal property measurement test are reported in Table 1, in association with the average temperature reached by the tissues.

Measurements in *ex vivo* liver samples were firstly performed to validate the adopted measurement technique, through a comparison with the results of other studies employing the dual-needle technique on hepatic tissue. The average values of thermal properties and the associated measurement uncertainty referring to the measurement repeatability are reported in Fig. 2.

Concerning the porcine hepatic tissue, a slight increase with temperature was observed for k, whose value was 0.571 ± 0.075 W/(m·K) at 65 °C. D presented a higher value at 65 °C (0.163 ± 0.029 mm^2/s) compared to the values at the other temperatures, while no specific correlation with increasing temperature was observed, at the considered temperatures, for c_v, whose values ranged from 3.48 ± 0.35 MJ/(m^3·K) to 3.70 ± 0.30 MJ/(m^3·K).

The results attained in this study are in accordance with the thermal properties measured in *ex vivo* ovine [20] and bovine [29] liver tissues as shown by the calculation of the percentage variation, expressed as in (5):

TABLE I. THERMAL PROPERTIES OF *EX VIVO* PORCINE LIVER AND KIDNEY TISSUES AND THE AGAR-BASED PHANTOM MEASURED BY THE DUAL-NEEDLE TECHNIQUE AT DIFFERENT SELECTED TEMPERATURES.

T [°C]	Porcine liver tissue								
	Thermal conductivity k [W/(m·K)]			Thermal diffusivity D [mm²/s]			Volumetric heat capacity c_v [MJ/(m³·K)]		
	Test 1	*Test 2*	*Test 3*	*Test 1*	*Test 2*	*Test 3*	*Test 1*	*Test 2*	*Test 3*
22	0.507	0.496	0.541	0.148	0.147	0.149	3.42	3.38	3.64
36	0.538	0.521	0.552	0.141	0.140	0.151	3.81	3.73	3.57
65	0.600	0.540	0.574	0.158	0.154	0.176	3.46	3.44	3.59
T [°C]	**Porcine kidney tissue**								
	Thermal conductivity k [W/(m·K)]			Thermal diffusivity D [mm²/s]			Volumetric heat capacity c_v [MJ/(m³·K)]		
	Test 1	*Test 2*	*Test 3*	*Test 1*	*Test 2*	*Test 3*	*Test 1*	*Test 2*	*Test 3*
25	0.546	0.568	0.572	0.150	0.152	0.151	3.65	3.73	3.78
36	0.560	0.579	0.585	0.153	0.155	0.155	3.65	3.73	3.78
60	0.550	0.566	0.566	0.161	0.157	0.156	3.41	3.61	3.64
T [°C]	**Agar-based phantom**								
	Thermal conductivity k [W/(m·K)]			Thermal diffusivity D [mm²/s]			Volumetric heat capacity c_v [MJ/(m³·K)]		
	Test 1	*Test 2*	*Test 3*	*Test 1*	*Test 2*	*Test 3*	*Test 1*	*Test 2*	*Test 3*
25	0.605	0.610	0.614	0.153	0.153	0.154	3.95	3.98	3.99
36	0.622	0.632	0.618	0.157	0.159	0.156	3.96	4.01	3.96
61	0.688	0.679	0.679	0.163	0.165	0.161	4.22	4.11	4.22

$$\%\ variation = \frac{|\overline{y_{T_{set}}} - \overline{y_{T_{reference}}}|}{\overline{y_{T_{reference}}}} \times 100 \qquad (5)$$

in which $\overline{y_{T_{set}}}$ is the arithmetic mean of the measurements performed at the temperature T_{set} in the present study, while $\overline{y_{T_{reference}}}$ is the arithmetic mean of the measurements reported in the reference literature study.

The percentage variations between the thermal properties measured at 22 °C in the present study and 25.35 °C in ovine liver [20] are 3.0%, 1.3%, and 2.7% for k, D, and c_v, respectively. Additionally, the percentage variations between the thermal properties measured at 21 °C in bovine liver tissue [29] and at 22 °C in the present study are 3.0%, 5.7%, and 0.3% for k, D, and c_v, accordingly. The trend of D is also in agreement with the measurements performed in porcine liver by Guntur *et al.*[34] who observed a lower value of D at a temperature close to body temperature compared to the value at room temperature, and a higher average D at 65 °C, compared to room and body temperatures.

While different studies focused on the thermal characterization of liver tissue of various species as a function of temperature [7], [19], [20], [29], [34], a limited number of investigations reported the thermal properties of other organs, such as kidney, as a function of temperature [27], [28]. In this regard, after the validation of the measurement method in liver tissue, we measured the thermal properties of porcine kidney tissue (Table 1). At an average temperature of 25 °C, the values of k, D, and c_v were 0.562 ± 0.035 W/(m·K), 0.151 ± 0.002 mm²/s, 3.72 ± 0.16 MJ/(m³·K), respectively. Close to body temperature (average temperature of 36 °C), kidney tissue was characterized by average values of k, D, and c_v equal to 0.575 ± 0.031 W/(m·K), 0.154 ± 0.003 mm²/s, and 3.72 ± 0.16 MJ/(m³·K), correspondingly. At higher temperatures (average value of 60 °C), k, D, and c_v of the *ex vivo* swine kidney tissue were 0.560 ± 0.023 W/(m·K), 0.158 ± 0.007 mm²/s, and 3.55 ± 0.31 MJ/(m³·K), accordingly. The measured thermal properties are comparable with the thermal properties attained by Silva *et al.*, who performed measurement adopting the dual-needle technique, in tissues of a different species, i.e., ovine kidney tissues, at room and body temperature [28] and up to ablative temperatures [27]. Overall, the observed higher uncertainty of liver tissues may be ascribable to the inter-sample variability and anisotropy characterizing the tissue specimens [7], [23].

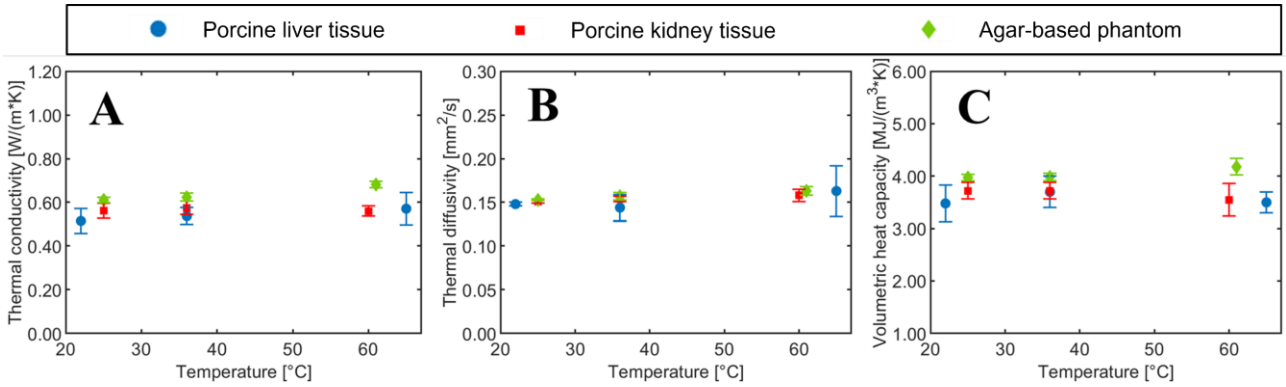

Fig. 2. Thermal conductivity (A), thermal diffusivity (B), and volumetric heat capacity (C) of *ex vivo* porcine liver and kidney tissues and the agar-based phantom measured as a function of the selected temperature values. The average values of the thermal properties and the associated measurement uncertainty are reported.

After the measurements in *ex vivo* biological tissue, we focused on the investigation of the thermal properties of an agar-based phantom, prepared to mimic soft tissue thermal properties [4], [5]. Tissue mimicking phantoms present several advantageous aspects for the study and optimization of medical therapies [4], [5], [30], [35], [36], as they can be realized with specific and tunable features according to the phenomenon one wants to investigate. Moreover, they can be prepared by adopting standard protocols, thus reducing the variability among different samples. The thermal properties of the agar-based phantom (Fig. 2) were compared to ones measured in *ex vivo* biological tissue, by calculating the percentage variation between the thermal properties measured for the phantom and for the *ex vivo* porcine kidney. Hence, the percentage variation was determined following the expression reported in (5), but in this case $\overline{y_{T_{set}}}$ was the thermal property of the phantom at a specific temperature and $\overline{y_{T_{reference}}}$ was the thermal property measured for *ex vivo* porcine kidney tissue. The percentage variations between the phantom and the tissue in terms of thermal diffusivity *D*, which describes the overall capability of the material to conduct heat in relation to its heat storage features, were 1.3%, and 1.9%, at average temperatures of 25 °C and 36 °C, respectively. Moreover, the percentage variation between the thermal diffusivity *D* measured at 61 °C in the agar phantom and at 60 °C in porcine kidney tissue was 3.2%. Hence, the phantom was able to well mimic this tissue thermal property, at the investigated temperatures.

IV. Conclusions

In this study, we present the results of the measurement of the thermal properties (i.e., *k*, *D*, and c_v) of *ex vivo* biological tissues, namely, porcine liver and kidney tissues at selected tissue temperatures (room temperature, close to body temperature and ~60 °C - 65 °C) with a dual-needle sensor. Furthermore, the thermal properties of an agar phantom were assessed by the same dual-needle technique at around the same temperature values. The results attained in *ex vivo* porcine liver validated the usage of the adopted method for the measurement of thermal properties in biological media. Besides, the measured thermal properties of porcine kidney tissue may be useful to better characterize its thermal behavior toward the amelioration of thermal treatments and their therapy planning. Further studies are required to expand the temperature interval in which the measurements are performed, as well as computationally and experimentally evaluate the influence of the physical properties and other important terms, such as blood perfusion, on the therapy outcome. Concerning the characterization of the phantom, the dual-needle sensors allowed for the measurements of its thermal properties and a comparison of the latter with the thermal properties of *ex vivo* biological tissue. The results validated the use of agar-based phantoms as tissue-mimicking materials and the employment of the dual-needle technique to assess their thermal properties, which is worthwhile for the final aim to attain materials with fine-tuned thermophysical properties.

Acknowledgment

This project has received funding from the European Research Council (ERC) under the European Union's Horizon 2020 research and innovation programme (Grant agreement No. 759159). This work was also funded by Fondazione Cariplo (grant n° 2017-2075). The authors would like to thank Mr. Ahad Mohammadi for supporting with the measurements on the liver tissue.

References

[1] M. A. El-Brawany, D. K. Nassiri, G. Terhaar, A. Shaw, I. Rivens, and K. Lozhken, "Measurement of thermal and ultrasonic properties of some biological tissues," J. Med. Eng. Technol., vol. 33, no. 3, pp. 249–256, Jan. 2009, doi: 10.1080/03091900802451265.

[2] J. R. Cook, R. R. Bouchard, and S. Y. Emelianov, "Tissue-mimicking phantoms for photoacoustic and ultrasonic imaging," Biomed. Opt. Express, vol. 2, no. 11, p. 3193, Nov. 2011, doi: 10.1364/BOE.2.003193.

[3] M. Lazebnik, E. L. Madsen, G. R. Frank, and S. C. Hagness, "Tissue-mimicking phantom materials for narrowband and ultrawideband microwave applications," Phys. Med. Biol., vol. 50, no. 18, pp. 4245–4258, Sep. 2005, doi: 10.1088/0031-9155/50/18/001.

[4] J. Cho, B. Prasad, and J. K. Kim, "Near-infrared laser irradiation of a multilayer agar-gel tissue phantom to induce thermal effect of traditional moxibustion," J. Innov. Opt. Health Sci., vol. 11, no. 06, p. 1850033, 2018.

[5] M. Zhang et al., "Experimental determination of thermal conductivity of water− agar gel at different concentrations and temperatures," J. Chem. Eng. Data, vol. 56, no. 4, pp. 859–864, 2011.

[6] S. Asadi et al., "Experimental Evaluation of Radiation Response and Thermal Properties of NPs-Loaded Tissues-Mimicking Phantoms," Nanomaterials, vol. 12, no. 6, p. 945, Mar. 2022, doi: 10.3390/nano12060945.

[7] C. Rossmann and D. Haemmerich, "Review of Temperature Dependence of Thermal Properties, Dielectric Properties, and Perfusion of Biological Tissues at Hyperthermic and Ablation Temperatures," Crit. Rev. Biomed. Eng., vol. 42, no. 6, pp. 467–492, 2014, doi: 10.1615/CritRevBiomedEng.2015012486.

[8] L. Bianchi, F. Cavarzan, L. Ciampitti, M. Cremonesi, F. Grilli, and P. Saccomandi, "Thermophysical and mechanical properties of biological tissues as a function of temperature: a systematic literature review," Int. J. Hyperth., vol. 39, no. 1, pp. 297–340, 2022, doi: 10.1080/02656736.2022.2028908.

[9] F. Izzo et al., "Radiofrequency Ablation and Microwave Ablation in Liver Tumors: An Update," Oncologist, vol. 24, no. 10, pp. e990–e1005, 2019, doi: https://doi.org/10.1634/theoncologist.2018-0337.

[10] M. G. Lubner, C. L. Brace, J. L. Hinshaw, and F. T. Lee, "Microwave Tumor Ablation: Mechanism of Action, Clinical Results, and Devices," J. Vasc. Interv. Radiol., vol. 21, no. 8, pp. S192–S203, Aug. 2010, doi: 10.1016/j.jvir.2010.04.007.

[11] S. Korganbayev et al., "Closed-Loop Temperature Control Based on Fiber Bragg Grating Sensors for Laser Ablation of Hepatic Tissue," Sensors, vol. 20, no. 22, p. 6496, Nov. 2020, doi: 10.3390/s20226496.

[12] L. Bianchi et al., "Thermal analysis of laser irradiation-gold nanorod combinations at 808 nm, 940 nm, 975 nm and 1064 nm wavelengths in breast cancer model," Int. J. Hyperth., vol. 38, no. 1, pp. 1099–1110, Jan. 2021, doi: 10.1080/02656736.2021.1956601.

[13] Y.-F. Zhou, "High intensity focused ultrasound in clinical tumor ablation," World J. Clin. Oncol., vol. 2, no. 1, p. 8, 2011, doi: 10.5306/wjco.v2.i1.8.

[14] J. P. Erinjeri and T. W. I. Clark, "Cryoablation: Mechanism of action and devices," Journal of Vascular and Interventional Radiology. 2010, doi: 10.1016/j.jvir.2009.12.403.

[15] K. F. Chu and D. E. Dupuy, "Thermal ablation of tumours: biological mechanisms and advances in therapy," Nat. Rev. Cancer, vol. 14, no. 3, pp. 199–208, Mar. 2014, doi: 10.1038/nrc3672.

[16] L. Bianchi, S. Korganbayev, A. Orrico, M. De Landro, and P. Saccomandi, "Quasi-distributed fiber optic sensor-based control system for interstitial laser ablation of tissue: theoretical and

experimental investigations," Biomed. Opt. Express, vol. 12, no. 5, p. 2841, May 2021, doi: 10.1364/BOE.419541.

[17] S. Singh and R. Melnik, "Thermal ablation of biological tissues in disease treatment: A review of computational models and future directions," Electromagn. Biol. Med., vol. 39, no. 2, pp. 49–88, Apr. 2020, doi: 10.1080/15368378.2020.1741383.

[18] A. Mohammadi, L. Bianchi, S. Korganbayev, M. De Landro, and P. Saccomandi, "Thermomechanical Modeling of Laser Ablation Therapy of Tumors: Sensitivity Analysis and Optimization of Influential Variables," IEEE Trans. Biomed. Eng., 2021, doi: 10.1109/TBME.2021.3092889.

[19] A. Mohammadi, L. Bianchi, S. Asadi, and P. Saccomandi, "Measurement of Ex Vivo Liver, Brain and Pancreas Thermal Properties as Function of Temperature," Sensors, vol. 21, no. 12, p. 4236, Jun. 2021, doi: 10.3390/s21124236.

[20] N. P. Silva, A. Bottiglieri, R. C. Conceição, M. O'Halloran, and L. Farina, "Characterisation of Ex Vivo Liver Thermal Properties for Electromagnetic-Based Hyperthermic Therapies," Sensors, vol. 20, no. 10, p. 3004, May 2020, doi: 10.3390/s20103004.

[21] P. Nesvadba, "A new transient method of the measurement of temperature dependent thermal diffusivity," J. Phys. D. Appl. Phys., vol. 15, no. 5, pp. 725–738, May 1982, doi: 10.1088/0022-3727/15/5/003.

[22] W. Buck and S. Rudtsch, "Thermal Properties," in Springer Handbook of Materials Measurement Methods, H. Czichos, T. Saito, and L. Smith, Eds. Berlin, Heidelberg: Springer Berlin Heidelberg, 2006, pp. 399–429.

[23] J. W. Valvano, J. R. Cochran, and K. R. Diller, "Thermal conductivity and diffusivity of biomaterials measured with self-heated thermistors," Int. J. Thermophys., vol. 6, no. 3, pp. 301–311, May 1985, doi: 10.1007/BF00522151.

[24] J. W. Valvano, J. T. Allen, and H. F. Bowman, "The Simultaneous Measurement of Thermal Conductivity, Thermal Diffusivity, and Perfusion in Small Volumes of Tissue," J. Biomech. Eng., vol. 106, no. 3, pp. 192–197, Aug. 1984, doi: 10.1115/1.3138482.

[25] I. V Agafonkina et al., "Thermal Properties of Human Soft Tissue and Its Equivalents in a Wide Low-Temperature Range," J. Eng. Phys. Thermophys., vol. 94, no. 1, pp. 233–246, Jan. 2021, doi: 10.1007/s10891-021-02292-y.

[26] T. Ackermann, "Book Review: Calorimetry. Fundamentals and Practice. By W. Hemminger and G. Höhne," Angew. Chemie Int. Ed. English, vol. 25, no. 5, pp. 482–483, May 1986, doi: https://doi.org/10.1002/anie.198604822.

[27] N. P. Silva, A. Bottiglieri, E. Porter, M. O'Halloran, and L. Farina, "Evaluation of Thermal Properties of Ex Vivo Kidney up to Ablative Temperatures," in IFMBE Proceedings, vol. 80, 2021, pp. 537–543.

[28] N. P. Silva, A. Bottiglieri, R. C. Conceicao, M. O'Halloran, and L. Farina, "Thermal Properties of Ex Vivo Biological Tissue at Room and Body Temperature," in 2020 14th European Conference on Antennas and Propagation (EuCAP), Mar. 2020, pp. 1–5, doi: 10.23919/EuCAP48036.2020.9135854.

[29] V. Lopresto, A. Argentieri, R. Pinto, and M. Cavagnaro, "Temperature dependence of thermal properties of ex vivo liver tissue up to ablative temperatures," Phys. Med. Biol., vol. 64, no. 10, p. 105016, May 2019, doi: 10.1088/1361-6560/ab1663.

[30] F. Morra et al., "Spatially resolved thermometry during laser ablation in tissues: Distributed and quasi-distributed fiber optic-based sensing," Opt. Fiber Technol., vol. 58, p. 102295, Sep. 2020, doi: 10.1016/j.yofte.2020.102295.

[31] L. Bianchi et al., "Fiber Bragg Grating Sensors-based Thermometry of Gold Nanorod-enhanced Photothermal Therapy in Tumor Model," IEEE Sens. J., 2021, doi: 10.1109/JSEN.2021.3082042.

[32] M. Abramowitz, I. A. Stegun, and R. H. Romer, "Handbook of Mathematical Functions with Formulas, Graphs, and Mathematical Tables," Am. J. Phys., vol. 56, no. 10, p. 958, Oct. 1988, doi: 10.1119/1.15378.

[33] I. E. C. BIPM, I. IFCC, I. ISO, and O. IUPAP, "Evaluation of measurement data—Guide to the expression of uncertainty in measurement. Joint Committee for Guides in Metrology, JCGM 100: 2008," Citado en las, pp. 18–21, 2008.

[34] S. R. Guntur, K. Il Lee, D.-G. Paeng, A. J. Coleman, and M. J. Choi, "Temperature-Dependent Thermal Properties of ex Vivo Liver Undergoing Thermal Ablation," Ultrasound Med. Biol., vol. 39, no. 10, pp. 1771–1784, Oct. 2013, doi: 10.1016/j.ultrasmedbio.2013.04.014.

[35] S. Curto et al., "Quantitative, multi-institutional evaluation of MR thermometry accuracy for deep-pelvic MR-hyperthermia systems operating in multi-vendor MR-systems using a new anthropomorphic phantom," Cancers (Basel)., vol. 11, no. 11, p. 1709, 2019.

[36] L. Farina, K. Sumser, G. van Rhoon, and S. Curto, "Thermal Characterization of Phantoms Used for Quality Assurance of Deep Hyperthermia Systems," Sensors, vol. 20, no. 16, 2020, doi: 10.3390/s20164549.